Mechanistic Studies of Thermolysin

Maria C. Izquierdo and Ross L. Stein*

Contribution from the Department of Enzymology, Merck Research Laboratories, P.O. Box 2000, RY 80N-A54, Rahway, New Jersey 07065. *Received February 12, 1990*

Abstract: To probe structural features of the rate-limiting transition state and the mechanistic origins of substrate specificity, we determined temperature dependencies and solvent and β-deuterium isotope effects for the thermolysin-catalyzed hydrolyses of FA-Gly-P′, where FA is 3-(2-furyl)acrylate and P′ is $AlaNH_2$, $AbuNH_2$, $ValNH_2$, $NvaNH_2$, $PheNH_2$, $LeuNH_2$, and Leu-Ala (cleavage occurs at Gly-P′). Important observations are (1) Eyring plots for k_c/K_m are nonlinear, with plateaus or decreases in activity at elevated temperatures. The following four reaction types are consistent with this result: (i) a simple reaction (i.e., a single rate-limiting transition state), with a negative heat capacity of activation; (ii) a complex reaction with partially rate-limiting, differentially temperature-sensitive sequential steps; (iii) a reaction involving a temperature-dependent equilibrium of two enzyme forms, where one form is inactive; and (iv) a reaction involving a temperature-dependent equilibrium of two enzyme forms, where both forms are active. Detailed analyses of the Eyring plots suggests that mechanism ii is most consistent with the data. (2) A plot of ln $[(k_c/K_m)_{T=5°C}]$ vs ln $[(k_c/K_m)_{T=20°C}]$ for the seven substrates of this study is linear and indicates that this series of reactions defines an isokinetic relationship. (3) k_c/K_m correlates with the hydrophobicity of the P_1' amino acid residue. (4) The β-deuterium isotope effect on k_c/K_m is 0.97 ± 0.01 for the hydrolyses of both FA-Gly-(L,L)-$LeuNH_2$ and FA-Gly-(L,L)-Leu-Ala (L = H, D) and suggests that the rate-limiting transition states for these reactions resemble the tetrahedral addition adduct of zinc-bound water and substrate. (5) For FA-Gly-$LeuNH_2$, the β-deuterium isotope effect increases with increasing temperature. (6) Solvent deuterium isotope effects on k_c/K_m for the hydrolyses of FA-Gly-P′ are all near 0.74 and indicate an absence of general-acid/general-base catalysis in the rate-limiting step. Combined, the results of this study suggest a sequential mechanism for thermolysin in which the Michaelis complex changes conformation prior to the chemical steps of peptide bond hydrolysis. k_c/K_m is rate-limited by both the conformational change and the hydrolysis step. The extent to which either of these steps limits k_c/K_m is dependent on temperature, with chemistry contributing more to rate limitation at lower temperature. The chemical step, which corresponds to formation and decomposition of a tetrahedral intermediate, is itself rate-limited by a reaction step that does not involve protolytic catalysis. Likely candidates for this step are addition of a zinc-bound hydroxide to the substrate carbonyl carbon and decomposition of a zwitterionic tetrahedral intermediate.

Introduction

The mechanism by which the metalloendoproteinase thermolysin catalyzes peptide bond hydrolysis remains the subject of intense investigation. A large body of X-ray crystallographic,[1-4] molecular modeling,[5] and kinetic work[6-11] exists for this enzyme. These studies have been motivated by the anticipation that the mechanism of thermolysin will be a paradigm for metalloproteinase catalysis and, thus, aid the design of mechanism-based inhibitors and provide a proving ground for investigators hoping to couple X-ray crystallography, molecular modeling, and kinetics.

A current view of the kinetic mechanism for thermolysin appears in Scheme I, where S is a peptide of general structure, RC(O)NHR′, and P and P′ are the reaction products, $RCOO^-$ and $^+H_3NR'$, respectively. This mechanism states that formation of the initial encounter complex of enzyme and substrate, $(E:S)_1$, is followed by production of the intermediate, $(E:S)_2$. Chemistry within $(E:S)_2$ then leads to the ternary complex of enzyme and two products. Release of products regenerates free enzyme in the final steps of the reaction.

The existence of an intermediate, $(E:S)_2$, is supported by the stopped-flow studies of Fukuda and Kunugi.[7b] These investigators observed a transient intermediate during the hydrolysis of FA-Gly-Phe-Ala[12] (cleavage at Gly-Phe) at pH values around 6 and suggested that this new species is a conformational isomer of $(E:S)_1$. In contrast, Morgan and Fruton[9] were unable to detect any new intermediate on the stopped-flow time scale during the hydrolysis of Mns-Phe-Leu-Ala (cleavage at Phe-Leu) at pH 8.5. We must conclude that accumulation of $(E:S)_2$ and possible rate limitation by reaction steps involving its formation or decomposition are dependent on structural features of the substrate and/or pH.

Scheme I. Proposal for the Kinetic Mechanism of Thermolysin

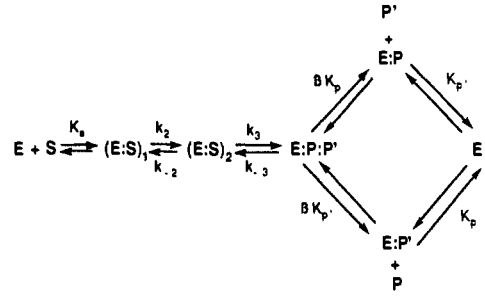

Scheme I shows random product release for thermolysin. This is supported by studies of Wayne and Fruton,[11] who demonstrated that for the hydrolysis of Z-Phe-Phe-OMe and Z-Phe-Phe-Gly-OMe (cleavage at Phe-Phe), product release is rapid-equilibrium random. However, Oyama and co-workers[13] showed that for the thermolysin-catalyzed hydrolysis of Z-Asp-Phe-OMe, product release is ordered with the amine product departing first. This order of release is consistent with the known ability of peptide carboxylate inhibitors to bind tightly to thermolysin.[5] Thus, the order of product release may be dependent on the structure of the two products.

The series of chemical steps that occurs within the active site and ultimately leads to peptide bond hydrolysis is still a matter of debate. It is known from X-ray crystallographic studies[2,4] that the active site of thermolysin contains a Zn^{2+}-bound water molecule and carboxylate and imidazole moieties of Glu_{143} and

(1) Holden, H. M.; Matthews, B. W. *J. Biol. Chem.* **1988**, *263*, 3256-3265.
(2) Kester, W. R.; Matthews, B. W. *Biochemistry* **1977**, *16*, 2506-2516.
(3) Monzing, A. F.; Matthews, B. W. *Biochemistry* **1984**, *23*, 5724-5729.
(4) Weaver, L. H.; Kester, W. R.; Matthews, B. W. *J. Mol. Biol.* **1977**, *114*, 119-132.
(5) Hangquer, D. G.; Monzingo, A. F.; Matthews, B. W. *Biochemistry* **1984**, *23*, 5730-5741.
(6) Feder, J.; Schuck, J. M. *Biochemistry* **1970**, *9*, 2784-2791.
(7) (a) Kunugi, S.; Hirohara, H.; Ise, N. *Eur. J. Biochem.* **1982**, *124*, 157-163. (b) Fukuda, M.; Kunugi, S. *Chem. Soc. Jpn.* **1984**, *57*, 2965-2970.
(8) Holmquist, B.; Vallee, B. L. *Biochemistry* **1976**, *15*, 101-107.
(9) Morgan, G.; Fruton, J. S. *Biochemistry* **1978**, *17*, 3562-3568.
(10) Stein, R. L. *J. Am. Chem. Soc.* **1988**, *110*, 7907-7908.
(11) Wayne, S. I.; Fruton, J. S. *Proc. Natl. Acad. Sci. U.S.A.* **1983**, *80*, 3241-3244.
(12) Abbreviations: FA, 3-(2-furyl)acryloyl; Abu, α-aminobutyric acid; Nva, norvaline; Mns, 6-(*N*-methylanilino)-2-naphthylene-1-sulfonyl; Z, carbobenzoxoyl.
(13) Oyama, K.; Kihara, K.; Nonaka, Y. *J. Chem. Soc. Perkin Trans. 2* **1981**, 356-360.

0002-7863/90/1512-6054$02.50/0

His_{231}, respectively. It is now generally thought that the Zn^{2+}–OH_2 serves as nucleophile in the direct attack of water on the substrate scissle bond, while the carboxylate and imidazole shuttle protons during the reaction.[5] Another mechanistic possibility that we should consider is that the carboxylate of Glu_{143} acts as a nucleophile with the generation of an anhydride acyl-enzyme intermediate. This has been observed for the hydrolysis of certain esters by the mechanistically related enzyme, carboxypeptidase A.[14] However, for thermolysin, O^{18}-labeling experiments of Antonov and co-workers[15] unambiguously demonstrated that peptide hydrolysis involves the direct attack of water with no involvement of an acyl-enzyme intermediate. Indirect studies of Bartlett and Marlowe[16] with peptide phosphonate inhibitors also support a mechanism involving attack of Zn^{2+}–OH_2. It appears, therefore, that thermolysin's active-site chemistry involves the attack of Zn^{2+}–OH_2 on the carbonyl carbon of the scissle bond to form a tetrahedral intermediate. Collapse of this species then leads to formation of the two products.

What have not been addressed in any of these studies are the related questions of which step is rate-limiting[17] and what is the structure of the rate-limiting transition state. The first study to probe these questions was a preliminary investigation from this laboratory, which studied the thermolysin-catalyzed hydrolysis of FA-Gly-$LeuNH_2$.[10] Solvent isotope effects (ratio of rate constants in H_2O and D_2O; abbreviated as ^{D_2O}k) and β-deuterium isotope effects (ratio of rate constants for the hydrolysis of FA-Gly-$LeuNH_2$ and FA-Gly(d_2)-$LeuNH_2$; abbreviated as $^{\beta D}k$) were determined and suggest that the process governed by k_c/K_m is rate-limited by one of the chemical steps of peptide bond hydrolysis; that is, formation or decomposition of the tetrahedral intermediate. We also found that this step is unaccompanied by general-acid/general-base catalysis.

In the work reported herein, we continue the theme developed in our earlier study and determine solvent and β-deuterium isotope effects for the thermolysin-catalyzed hydrolysis of FA-Gly-Leu-Ala. Our interest in this substrate lies in the 30-fold enhancement of k_c/K_m relative to k_c/K_m for the hydrolysis of FA-Gly-$LeuNH_2$. Our aim is to probe the mechanistic origins of this rate constant-enhancement.

Additional mechanistic insight into catalysis by thermolysin will be sought through temperature-dependence studies. We will examine FA-Gly-Leu-Ala as well as the series of substrates, FA-Gly-P_1'-NH_2, where P_1'[18] is Ala, Abu, Nva, Val, Phe, and Leu. Our investigation of the temperature dependence of these reactions was not only motivated by the general utility of such studies in mechanistic chemistry but also by earlier observations of severely nonlinear Erying plots for the hydrolysis of FA-Gly-$LeuNH_2$ and FA-Gly-$PheNH_2$.[7a] Although these investigators noted the nonlinearity of their plots, they gave no mechanistic rationale for it. In the present work, we not only reproduce nonlinear Erying plots for FA-Gly-$LeuNH_2$ and FA-Gly-$PheNH_2$ but also find that the thermolysin-catalyzed hydrolyses of *all* members of this series, as well as FA-Gly-Leu-Ala, have temperature dependencies that yield nonlinear Erying plots.

(14) Suh, J.; Hong, S.-B.; Chung, S. *J. Biol. Chem.* **1986**, *261*, 7112–7114.
(15) Antonov, V. K.; Ginodman, L. M.; Rumsh, L. D.; Kapitannikov, Y. V.; Barshevskaya, T. N.; Yavashev, L. P.; Gurova, A. G.; Volkova, L. I. *Eur. J. Biochem.* **1981**, *117*, 195–200.
(16) Bartlett, P. A.; Marlowe, C. K. *Biochemistry* **1983**, *22*, 4618–4624.
(17) As O'Leary has recently pointed out (*Annu. Rev. Biochem.* **1989**, *58*, 377–401), there is no generally agreed upon definition for the term "rate-determining" or "rate-limiting" step. In this paper, we are primarily concerned with elucidating structural features of the "rate-limiting transition state" for the enzymic process that is governed by the steady-state kinetic term k_c/K_m. In this paper, "rate-limiting transition state" will refer to the transition state of highest free energy and, by analogy, "rate-limiting step" will refer to that reaction step that has the highest free energy. Where several transition states have similar free energies, these steps will be said to be "partially rate-limiting". The composite transition state that is experimentally accessible in a reaction having several "partially rate-limiting steps" will be referred to as a "virtual transition state".[25,26]
(18) The nomenclature for the amino acid residues of the substrate (P_n-...P_3-P_2-P_1-P_1'-P_2'-P_3'-...-P_n) and the corresponding protease subsites (S_n-...S_2-S_1-S_1'-S_2'-S_3'-...-S_n) is that of Schecter and Berger (*Biochem. Biophys. Res. Commun.* **1967**, *27*, 157–162). Hydrolysis occurs at the P_1–P_1' bond.

Table I. Specificity of Thermolysin for Substrates of Structure FA-Gly-P'[a]

P'	[E], μM	[S], μM	k_c/K_m,[b] M^{-1} s^{-1}
$AlaNH_2$	40	1,000	45
$AbuNH_2$	8	100	410
$ValNH_2$	8	100	1,250
$NvaNH_2$	1.5	100	3,240
$PheNH_2$	0.3	100	15,700
$LeuNH_2$	0.3	100	17,700
Leu-Ala	0.022	20	620,000

[a] Reaction conditions: 100 mM MES, 10 mM $CaCl_2$, pH 6.48, 25.1 °C. [b] Error limits are less than 10% in all cases.

Table II. Steady-State Kinetic Parameters for Thermolysin Catalysis[a]

substrate	K_m, mM	k_c, s^{-1}	k_c/K_m, M^{-1} s^{-1}
FA-Gly-$LeuNH_2$[b]	≥30	≥650	21 600
FA-Gly-Leu-Ala[c]	0.22	140	630 000

[a] Reaction conditions: 100 mM MES, 10 mM $CaCl_2$, pH 6.48, 25.1 °C. [b] $0.10 \le [S]_0 \le 5.0$ mM; $[E]_0 = 0.17$ μM. [c] $0.14 \le [S]_0 \le 2.2$ mM; $[E]_0 = 0.022$ μM.

Experimental Section

Reagents. Buffer salts and deuterium oxide were from Sigma Chemical Co. All substrates were prepared by Bachem. The deuterated substrates met our criteria for chemical, isotopic, and kinetic purity discussed previously.[10] Thermolysin was purchased form Calbiochem and prepared as a 3 mg/mL stock solution in pH 7.5 buffer containing 0.10 M HEPES, 0.01 M $CaCl_2$, and 2.5 M NaBr. Buffers for the solvent isotope effect studies were prepared as described previously.[19,20]

Kinetic Experiments. In a typical kinetic run, 2.80 mL of buffer and 0.10 mL of substrate in DMSO were added to a 3-mL cuvette, and the cuvette was placed in the jacketed cell holder of an Aviv Model 14DS spectrophotometer. Temperature of reaction solutions was kept constant (±0.02 °C) by water circulated from a Brinkman RM6 water bath. Using an Omega thermistor thermometer, we continuously monitored the temperature of a water-filled cuvette that was placed in the cell holder adjacent to the reaction solution. After the reaction solution had reached thermal equilibrium (≥15 min), we initiated the reaction by addition of 0.10 mL of enzyme stock solution. Reaction progress was monitored by the absorbance change at 322 nm ($\Delta\epsilon = -2300$) that accompanies cleavage of FA-Gly-X at the Gly-X bond. For each kinetic run, between 600 and 1000 data points, corresponding to {time, OD_{322}} pairs, were collected by an AT&T PC 6300 microcomputer interfaced to the spectrophotometer.

Data Analysis. To obtain k_c/K_m, reaction progress curves were recorded under the condition $[S] \ll K_m \gg [E]$. These curves were first order in substrate and were fit to a simple first-order rate law to obtain the observed first-order rate constant, k_{obs}. Division of k_{obs} by [E] gave k_c/K_m. To obtain k_c and K_m, we either determined initial velocities at various substrate concentrations and fit these data to the Michaelis–Menten equation or recorded entire reaction progress curves at $[S] > K_m$ and fit the instantaneous velocity vs substrate concentration data to the Michaelis–Menten equation. Analysis programs were written by Dr. P. Huskey (Rutgers University).

Determination of Isotope Effects. Each isotope effect that we report represents the mean and standard deviation for the combined results of two or three independent isotope effect experiments. Each of these experiments involved five to eight individual isotope effect measurements, where each isotope effect measurement is the ratio of two kinetic runs: $^{H}k_{obs}/^{D}k_{obs}$.

Results

Steady-State Kinetic Parameters for Thermolysin Catalysis. Since at pH values near neutrality, K_m values for thermolysin substrates of structure, FA-Gly-P_1'-NH_2, are generally greater than 10^{-2} M,[7a,21] the only kinetic parameter that can be determined is k_c/K_m. These values and k_c/K_m for FA-Gly-Leu-Ala were determined at pH 6.48 and 25.1 °C and are collected in Table

(19) Stein, R. L.; Elrod, J. P.; Schowen, R. L. *J. Am. Chem. Soc.* **1983**, *105*, 2446–2452.
(20) Stein, R. L.; Strimpler, A. M.; Hori, H.; Powers, J. C. *Biochemistry* **1987**, *26*, 1305–1314.
(21) Feder, J. *Biochem. Biophys. Res. Commun.* **1968**, *32*, 326–332.

Table III. Kinetic Secondary β-Deuterium Isotope Effects for Thermolysin Catalysis[a]

substrate	pH	$^{\beta D}(k_c/K_m)$
FA-Gly-LeuNH$_2$[b]	6.48	0.978 ± 0.013
	7.57	0.961 ± 0.016
FA-Gly-Leu-Ala[c]	6.48	0.968 ± 0.012
	7.57	0.976 ± 0.007

[a] For the studies at pH 6.48, a buffer containing 100 mM MES was used, while for the studies at pH 7.57, a 100 mM HEPES buffer was used. Both solution also contained 10 mM $CaCl_2$. T = 25 ± 0.02 °C. [b] [S] = 100 μM; [E] = 0.30 μM. [c] [S] = 20 μM; [E] = 0.020 μM.

I. Similar results were reported in an earlier study by Pank and co-workers.[22] As originally observed by Morihora and Tsuzuki[23] for the series Z-Gly-P_1'-NH$_2$, reactivity as measured by k_c/K_m positively correlates with bulk and/or hydrophobicity of the P_1' residue. Extending the substrate to FA-Gly-Leu-Ala is also accompanied by an increase in k_c/K_m and indicates an important transition-state-stabilizing interaction at S_2'.

In contrast to FA-Gly-LeuNH$_2$, the K_m for the reaction of FA-Gly-Leu-Ala with thermolysin at pH values less than 7 is below 10^{-3} M. Initial velocities were determined at concentrations of FA-Gly-Leu-Ala ranging from 0.14 to 2.2 mM (data not shown) and were fit to the Michaelis–Menten equation to provide the steady-state kinetic parameters given in Table II. Initial velocities were also determined as a function of the concentration of FA-Gly-LeuNH$_2$. Both the double-reciprocal plot and the plot of v_0 vs $[S]_0$ for this substrate intersect at the origin and indicate that even the highest concentration of substrate, 5 mM, is still much less than K_m. On the basis of this observation, we can set a conservative lower limit for K_m of 30 mM. This value agrees with previous estimates of K_m for this substrate.[6] With this lower limit for K_m and a value for k_c/K_m, we can calculate a lower limit for k_c. These values are also summarized in Table II.

Interestingly, k_c for FA-Gly-LeuNH$_2$ is at least 6-fold greater than k_c for FA-Gly-Leu-Ala and indicates that the 30-fold increase in k_c/K_m that is associated with increasing the length of FA-Gly-LeuNH$_2$ to FA-Gly-Leu-Ala is due to a 150-fold decrease in K_m. As we discuss below, we believe that this decrease in K_m is not due to a decrease in K_s (see Scheme I) that would accompany stabilization of $(E:S)_1$ but, rather, is due to the accumulation of a reaction intermediate that occurs subsequent to $(E:S)_1$, such as $(E:S)_2$.

Isotope Effects for Thermolysin Catalysis. To probe the mechanistic origins of the rate enhancement that is observed when FA-Gly-LeuNH$_2$ is extended to FA-Gly-Leu-Ala, β-deuterium and solvent deuterium isotope effects were determined for the thermolysin-catalyzed hydrolysis of these two substrates. The β-deuterium isotope effects are collected in Table III and can be seen to have no detectable dependence on substrate structure or pH. An overall average value of 0.97 ± 0.01 can be calculated from these data. Solvent deuterium isotope effects on k_c/K_m for the thermolysin-catalyzed hydrolyses of FA-Gly-P′ (P′ = AlaNH$_2$, AbuNH$_2$, ValNH$_2$, NvaNH$_2$, PheNH$_2$, LeuNH$_2$, and Leu-Ala) are collected in Table IV. These values are all near 0.74.

Temperature Dependence of Thermolysin Catalysis. For the substrate series, FA-Gly-P′ (P′ = AlaNH$_2$, AbuNH$_2$, ValNH$_2$, NvaNH$_2$, PheNH$_2$, and LeuNH$_2$,), values of k_c/K_m were determined at several temperatures between 5 and 60 °C. The results are summarized in Table V and expressed in Figure 1 as Eyring plots of ln $[k'(h/k^*T)]$ vs $1/T$, where h is Planck's constant, k^* is Boltzmann's constant, T is expressed in degrees Kelvin, and k' is a pseudo-first-order rate constant obtained by multiplying k_c/K_m by a standard-state enzyme concentration of 10^{-6} M. In ideal cases, where linear Eyring plots are observed, the enthalpy of activation can be obtained from the slope, $-\Delta H^{\ddagger}/R$, and the entropy of activation obtained from the y intercept, $\Delta S^{\ddagger}/R$, where

Table IV. Kinetic Solvent Deuterium Isotope Effects on k_c/K_m for Thermolysin-Catalyzed Hydrolyses of Substrates of Structure FA-Gly-P′[a,b]

P′	solvent isotope effect	P′	solvent isotope effect
AlaNH$_2$	0.80 ± 0.01	PheNH$_2$	0.73 ± 0.02
AbuNH$_2$	0.73 ± 0.01	LeuNH$_2$	0.69 ± 0.02
ValNH$_2$	0.76 ± 0.01	Leu-Ala	0.72 ± 0.01
NvaNH$_2$	0.73 ± 0.01		

[a] Reaction conditions: 100 mM MES, 10 mM $CaCl_2$, pH 6.48, 25.1 ± 0.05 °C. [b] Initial conditions: substrate ($[S]_0$, $[E]_0$); Ala-NH$_2$, (1.0 mM, 40 μM); Abu-NH$_2$ (0.10 mM, 8.0 μM); Val-NH$_2$ (0.10 mM, 8.0 μM); Nva-NH$_2$ (0.10 mM, 1.5 μM); Phe-NH$_2$ (0.10 mM, 0.30 μM); Leu-NH$_2$ (0.10 mM, 0.30 μM); Leu-Ala (0.020 mM, 0.022 μM).

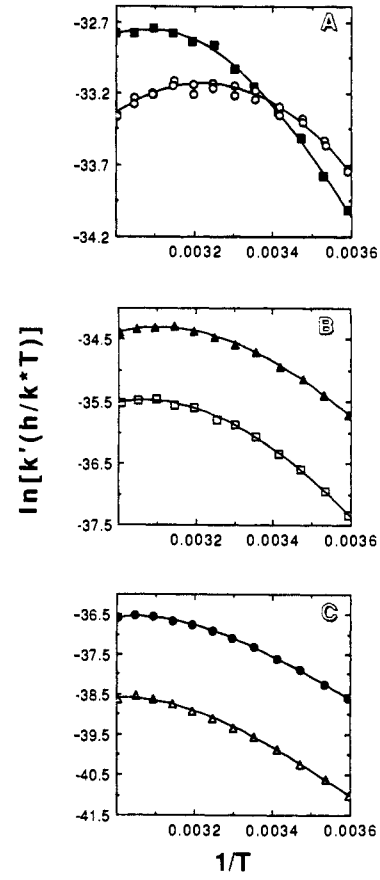

Figure 1. Temperature dependence of thermolysin catalysis. Eyring plots were constructed from values of k_c/K_m normalized to a standard-state enzyme concentration of 10^{-6} M. Reactions were conducted in a pH 6.48 buffer containing 100 mM MES and 10 mM $CaCl_2$. (A) FA-Gly-LeuNH$_2$ (filled squares) and FA-Gly-PheNH$_2$ (circles). (B) FA-Gly-NvaNH$_2$ (filled triangles) and FA-Gly-ValNH$_2$ (squares). (C) FA-Gly-AbuNH$_2$ (filled circles) and FA-Gly-AlaNH$_2$ (triangles). In all cases, the lines through the data points were drawn from the parameters of Table VIII and the thermodynamic equation based on eq 17.

R is the gas constant. In all of the present cases, however, the Eyring plots are severely nonlinear and do not allow simple analysis or interpretation. Mechanisms that account for this nonlinearity are discussed below.[24]

(22) Pank, M.; Kirret, O.; Paberit, N.; Aaviksaar, A. *FEBS Lett.* **1982**, *142*, 297–300.

(23) (a) Morihara, K.; Tsuzuki, H. *Eur. J. Biochem.* **1970**, *15*, 374–380. (b) Morihara, K. *Annu. Rev. Biochem.* **1971**, *41*, 179–243.

(24) Two trivial explanations for the curved Eyring plots can be dismissed: enzyme denaturation and temperature-dependent changes in pK_a values of active-site residues. We eliminated enzyme denaturation as a possible cause of the curved Eyring plots with experiments in which a solution of thermolysin was first incubated at 60 °C (the highest temperature used in our experiments) for 30 min (twice the normal time required to collect a reaction progress curve). The enzyme solution was then cooled and assayed at 25 °C and found to have an activity that was identical with the activity of enzyme that had never seen 60 °C. We dismissed the second possibility on the basis of the work of Kunugi and co-workers.[7a] These investigators demonstrated that the temperature dependence of the pH of the assay buffer (0.1 M MES, 0.01 M $CaCl_2$, pH 6.8 at 25 °C) is the same as the temperature dependence of the pH of maximum activity on the pH vs k_c/K_m profile.

Table V. Values of k_c/K_m as a Function of Temperature for the Thermolysin-Catalyzed Hydrolysis of FA-Gly-P′ [a,b]

P′	T (°C), k_c/K_m (M^{-1} s^{-1})
Ala-NH_2	5.0, 8.7; 9.8, 13.3; 14.9, 19.7; 20.0, 28.5; 25.2, 40.0; 30.0, 50.5; 35.0, 65.3; 40.0, 80.0; 45.1, 95.8; 50.1, 109; 54.9, 121; 59.9, 113
Abu-NH_2	5.1, 99.0; 10.0, 140; 15.0, 205; 20.0, 273; 25.3, 384; 30.2, 475; 35.0, 580; 40.2, 695; 45.1, 781; 50.1, 886; 55.1, 911; 60.0, 870
Val-NH_2	5.0, 349; 10.0, 524; 15.0, 746; 19.1, 993; 25.0, 1330; 29.8, 1640; 34.2, 1810; 40.0, 2250; 44.9, 2360; 49.9, 2660; 54.8, 2630; 59.7, 2550
Nva-NH_2	4.9, 1770; 10.1, 2460; 14.6, 3230; 19.5, 4010; 25.0, 5120; 29.8, 5930; 34.8, 6670; 39.9, 7600; 44.9, 8270; 50.1, 8330; 55.2, 8200; 59.9, 7870
Phe-NH_2	5.2, 13200; 10.2, 15900; 14.7, 18800; 19.6; 19600; 25.1, 23500; 29.8, 24700; 35.0, 25700; 39.6, 24100; 44.6, 26800; 50.0, 25000; 55.1, 24700; 60.0, 21800
	5.5, 126; 9.8, 15300; 14.6, 18200; 19.6, 20700; 25.0, 22300; 29.7, 23000; 34.9, 24800; 39.8, 25700; 45.0, 26000; 50.2, 24900; 50.3, 25100; 55.4, 23700; 60.0, 22100; 60.0, 22000
Leu-NH_2	5.1, 9630; 10.5, 12400; 14.9, 16400; 19.9, 20100; 25.3, 24100; 29.7, 28000; 34.7, 33700; 40.0, 35000; 45.0, 37700; 50.0, 39700; 55.1, 39000; 60.0, 39000

[a] Reaction conditions: 100 mM MES, 0.010 mM $CaCl_2$, 3% DMSO, pH 6.48. [b] Initial conditions: substrate ($[S]_0$, $[E]_0$); Ala-NH_2, (1.0 mM, 40 μM); Abu-NH_2 (0.10 mM, 8.0 μM); Val-NH_2 (0.10 mM, 8.0 μM); Nva-NH_2 (0.10 mM, 1.5 μM); Phe-NH_2 (0.10 mM, 0.30 μM); Leu-NH_2 (0.10 mM, 0.30 μM).

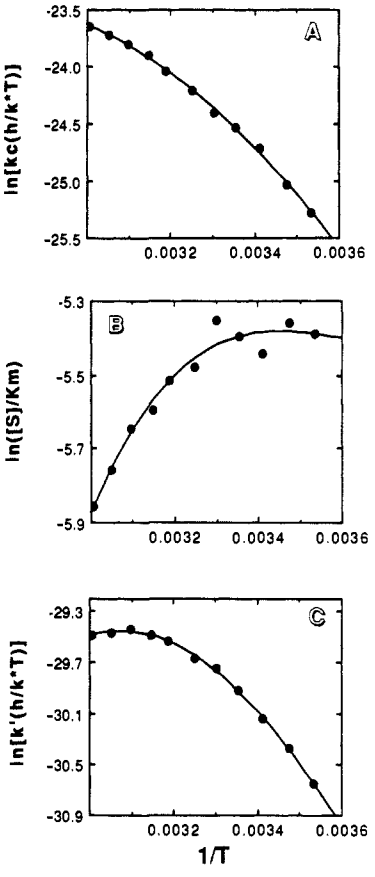

Figure 2. Temperature dependence of steady-state kinetic parameters for the thermolysin-catalyzed hydrolysis of FA-Gly-Leu-Ala. Reactions were conducted in a pH 6.48 buffer containing 100 mM MES and 10 mM $CaCl_2$. k_c (A) was used directly in its Eyring plot; K_m (B) was inverted to convert it to an assiciation constant and multiplied by $[S]_{standard\text{-}state} = 10^{-6}$ M before plotting; and k_c/K_m (C) was multiplied by $[E]_{standard\text{-}state} = 10^{-6}$ M before plotting. The lines through the data points were drawn for k_c (A) and k_c/K_m (C) from the parameters of Table VIII and the thermodynamic equations based on eq 15 and 17, respectively. The line through the K_m data of (B) is the best-fit third-degree polynomial and was included to aid the eye.

In contrast to substrates of the series, FA-Gly-X-NH_2, where K_m is greater than 10^{-2} M, the K_m for FA-Gly-Leu-Ala is less than 10^{-3} M. This allowed us to determine the temperature dependence of the individual steady-state parameters, k_c, K_m, and k_c/K_m, from full progress curves recorded at $[S]_0 = 2K_m$ and various temperatures. In preliminary experiments, at 25 °C, we demonstrated that steady-state parameters obtained by this method are essentially identical with those obtained from initial velocity studies (data not shown). Eyring plots of the data for k_c and k_c/K_m appear in parts a and c of Figure 2, respectively, and the van't Hoff plot of the K_m data appears in Figure 2b. For the van't Hoff plot, the steady-state association constant, $1/K_m$, was multiplied by a standard-state substrate concentration of 10^{-6} M.

We also determined β-deuterium and solvent deuterium isotope effect on k_c/K_m for the thermolysin-catalyzed hydrolysis of FA-Gly-LeuNH$_2$ at 5, 25, and 60 °C. These values are summarized in Table VI. While the β-deuterium isotope effect increases with increasing temperature, the solvent isotope effects show a minimum with temperature.

Table VI. Temperature Dependence of Kinetic Isotope Effects for the Thermolysin-Catalyzed Hydrolysis of FA-Gly-Leu-NH_2[a]

T, °C	$^{\beta D}(k_c/K_m)$[b]	$^{D_2O}(k_c/K_m)$[c]
5	0.966 ± 0.008	0.74 ± 0.01
25	0.978 ± 0.013	0.69 ± 0.02
60	0.986 ± 0.016	0.78 ± 0.02

[a] [S] = 100 μM; [E] = 0.30 μM. [b] 100 mM MES, 0.01 $CaCl_2$, pH 6.48. [c] 100 mM MES, 0.01 $CaCl_2$, pH 6.48 and pD equivalent.[37]

Scheme II. Kinetic Mechanisms for Thermolysin

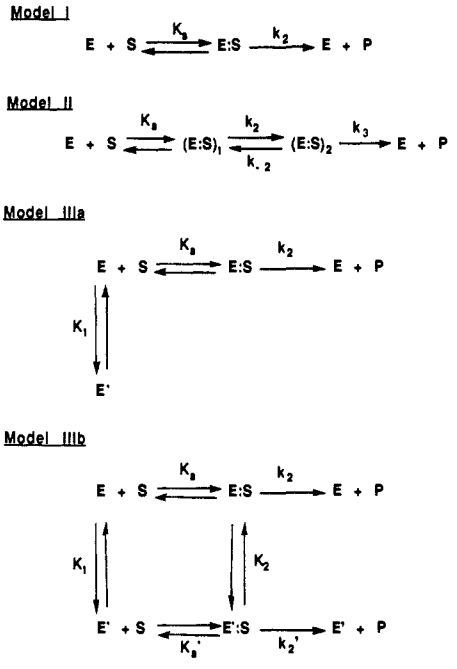

Theory: Models for the Temperature Dependence of Thermolysin

Curved Eyring plots of the sort that we observe in this study can arise from only two general reaction types;[27] a kinetically

(25) Schowen, R. L. In *Transition States of Biochemical Processes*; Gandour, R. D., Schowen, R. L., Eds.; Plenum Press: New York, 1978.
(26) Stein, R. L. *J. Org. Chem.* **1981**, *46*, 3328-3330.
(27) Blandamer, M. J.; Burgess, J.; Robertson, R. E.; Scott, J. M. W. *Chem. Rev.* **1982**, *82*, 259-286.

simple, one-step reaction that has a nonzero heat capacity of activation ($\Delta C_p^{\ddagger}$) or a kinetically complex, multistep reaction that is characterized by differentially heat sensitive sequential or parallel steps, where $\Delta C_p^{\ddagger}$ for the various steps is assumed to be zero. In enzymic reactions, these two general cases can be expanded to the four models that are shown in Scheme II.

In this section, we will consider each of these models in an attempt to see which one best accounts for our data.[24]

Model I: Single Transition State with a Nonzero $\Delta C_p^{\ddagger}$. Model I is the simplest expression for thermolysin kinetics. We will show that the only way this model can produce curved Eyring plots is if the heat capacity of activation is nonzero.

Under the conditions of our temperature-dependence studies, where $[S] \ll K_m$, the initial velocity expression for the mechanism of model I is given by eq 1:

$$\frac{-d[S]}{dt} = \frac{k_2}{K_s}[E]_0[S]_0 \tag{1}$$

If this equation is integrated with respect to [S]

$$[S] = [S]_0 \exp(-k_{obs}t) \tag{2}$$

where

$$k_{obs} = \frac{k_2}{K_s}[E]_0 \tag{3}$$

Equation 3 can be recast in the thermodynamic terms of transition-state theory as shown:

$$k_{obs} = \frac{k^*T}{h} \exp\left(\frac{-\Delta G^{\ddagger}_{obs}}{RT}\right) \tag{4}$$

Since

$$\Delta G^{\ddagger}_{obs} = \Delta G^{\ddagger}_2 - \Delta G_s \tag{5}$$

where $\Delta G^{\ddagger}_2$ is the energy of activation for the process governed by k_2 and ΔG_s is the free energy difference corresponding to K_s, eq 4 can be rewritten as

$$k_{obs} = \frac{k^*T}{h} \exp\left(-\frac{\Delta G^{\ddagger}_2 - \Delta G_s}{RT}\right) \tag{6}$$

This expression can be expanded to

$$k_{obs} = \frac{k^*T}{h} \exp\left[-\frac{[(\Delta H^{\ddagger}_2 - \Delta H_s) - T(\Delta S^{\ddagger}_2 - \Delta S_s)]}{RT}\right] \tag{7}$$

If this is now rewritten in a form suitable for an Eyring plot, we obtain

$$\ln\left(k_{obs}\frac{h}{k^*T}\right) = -\frac{\Delta H^{\ddagger}_2 - \Delta H_s}{R}\frac{1}{T} + \frac{\Delta S^{\ddagger}_2 - \Delta S_s}{R} \tag{8}$$

Thus, if the mechanism of model I was operating in its simplest thermodynamic form, the Erying plot of $\ln [k_{obs}(h/k^*T)]$ vs $1/T$ would be linear with a slope and intercept of $-(\Delta H^{\ddagger}_2 - \Delta H_s)/R$ and $(\Delta S^{\ddagger}_2 - \Delta S_s)/R$, respectively. We see then that the only way in which a curved Erying plot can be obtained for the mechanism of model I is if the heat capacity for either K_s or k_2 is not equal to zero.

The expression for $\Delta G^{\ddagger}_{obs}$ that includes a heat capacity term is given below:[28]

$$\Delta G^{\ddagger}_{obs} = (\Delta H^{\ddagger}_{obs} - T\Delta C_p^{\ddagger}{}_{obs}) - T[\Delta S^{\ddagger}_{obs} - (\ln T)\Delta C_p^{\ddagger}{}_{obs}] \tag{9}$$

where

$$\Delta C_p^{\ddagger}{}_{obs} = \Delta C_p^{\ddagger}{}_2 - \Delta C_{p,s} \tag{10}$$

Values of $\Delta X^{\ddagger}_{obs}$ ($X = H, S, C_p$) were determined by fitting the dependence of $\Delta G^{\ddagger}_{obs}$ on T to the simple, second-degree polynomial:

$$\Delta G^{\ddagger}_{obs} = a + bT + cT^2 \tag{11}$$

$\Delta C_p^{\ddagger}{}_{obs}$, $\Delta H^{\ddagger}_{obs}$, and $\Delta S^{\ddagger}_{obs}$ were then calculated according to eqs 12–14:

$$\Delta C_p^{\ddagger}{}_{obs} = -2cT \tag{12}$$

$$\Delta H^{\ddagger}_{obs} = (a - cT^2) - T\Delta C_p^{\ddagger}{}_{obs} \tag{13}$$

$$\Delta S^{\ddagger}_{obs} = (-b - 2cT) - (\ln T)\Delta C_p^{\ddagger}{}_{obs} \tag{14}$$

For this analysis, $\Delta G^{\ddagger}_{obs}$ values were generated from eqs 3 and 4 in which $[E]_0$ was first set equal to a standard-state concentration of 10^{-6} M. k_2/K_s values were the experimentally determined values of k_c/K_m summarized in Table V.

Values of $\Delta H^{\ddagger}_{obs}$, $\Delta S^{\ddagger}_{obs}$, and $\Delta C_p^{\ddagger}{}_{obs}$ for thermolysin-catalyzed hydrolyses are summarized in Table VII. The $\Delta H^{\ddagger}_{obs}$ and $\Delta S^{\ddagger}_{obs}$ values indicate enormous increases in energy and disorder as the transition state for the process that is governed by k_2/K_s is reached. These values are not unlike the ΔH and ΔS values that are observed when proteins denature.[28] In contrast, the large negative values of $\Delta C_p^{\ddagger}{}_{obs}$ can be interpreted in terms of a transition-state structure where hydrophobic groups are exposed less to solvent than in the ground state[28,29] and are reminiscent of protein refolding.

We see from this analysis that activation parameters that are calculated according to model I suggest large-scale protein conformational changes that are usually associated with protein folding. It is unlikely that activation parameters of this magnitude could result from entry of an enzyme and substrate into their catalytic transition state. Thus, model I need not be considered as a likely candidate in explaining the temperature dependencies that we observe.

Table VII. Activation Parameters[a] for the Thermolysin-Catalyzed Hydrolysis of FA-Gly-P′: Analysis According to Model I

P′	$\Delta H^{\ddagger}_{obs}$	$\Delta S^{\ddagger}_{obs}$	$\Delta C_p^{\ddagger}{}_{obs}$
Ala-NH_2	80	1300	−240
Abu-NH_2	80	1300	−240
Val-NH_2	87	1500	−270
Nva-NH_2	76	1300	−240
Phe-NH_2	56	960	−180
Leu-NH_2	65	1100	−200

[a] Units: $\Delta H^{\ddagger}_{obs}$, kcal/mol; $\Delta S^{\ddagger}_{obs}$ and $\Delta C_p^{\ddagger}{}_{obs}$, cal/mol·K.

Model II: Complex Reaction with Sequential, Differentially Temperature-Sensitive Steps. Model II is a simplification of the mechanism of Scheme II. The product release steps have been omitted since our reactions were conducted in the absence of added product. Furthermore, the concentration of any product that does accumulate during the course of reaction will be much less than the dissociation constants for the various enzyme–product complexes. The rate constant for synthesis of the peptide bond, k_{-3}, has also been omitted since k_{-3} is essentially zero when P is FA-Gly.[11] The mechanism of model II will produce curved Erying plots if the rate constants are differentially temperature-sensitive.

The steady-state rate expressions that describe the mechanism of model II are shown in eqs 15–17. In these equations, K_2

$$k_c = \frac{k_3}{1 + K_2(1 + \alpha)} \tag{15}$$

$$K_m = K_sK_2\left[\frac{1 + \alpha}{1 + K_2(1 + \alpha)}\right] \tag{16}$$

$$\frac{k_c}{K_m} = \frac{k_2}{K_s}\left[\frac{\alpha}{1 + \alpha}\right] \tag{17}$$

($=k_{-2}/k_2$) is the equilibrium constant for the reversible conversion of $(E{:}S)_1$ and $(E{:}S)_2$, and $\alpha(=k_3/k_{-2})$ is the forward-to-reverse

(28) Cantor, C. R.; Schimmel, P. R. *Biophysical Chemistry, The Behavior of Biological Macromolecules*; W. H. Freeman and Co.: New York, 1980; Part III, pp 1075–1105.

(29) Pace, N. C.; Tanford, C. *Biochemistry* **1968**, *7*, 198–208.

Table VIII. Activation Parameters[a,b] for the Thermolysin-Catalyzed Hydrolysis of FA-Gly-P′: Analysis According to Model II

P′	$\Delta H^{\ddagger}_{III}$	$\Delta S^{\ddagger}_{III}$	$\Delta H^{\ddagger}_{II}$	$\Delta S^{\ddagger}_{II}$	ΔH_{α}	ΔS_{α}
$AlaNH_2$	13.6 ± 0.8	−33.0 ± 3.2	−0.5 ± 0.3	−78.0 ± 7.2	14.1 ± 1.3	45.1 ± 4.1
$AbuNH_2$	12.0 ± 0.4	−34.2 ± 1.4	−4.3 ± 1.5	−85.5 ± 5.3	16.3 ± 1.5	51.3 ± 5.3
$ValNH_2$	14.8 ± 0.8	−21.5 ± 2.9	−0.9 ± 0.8	−73.5 ± 2.9	15.7 ± 1.2	52.0 ± 4.7
$NvaNH_2$	12.3 ± 0.8	−27.0 ± 3.1	−2.3 ± 1.0	−75.6 ± 2.9	14.6 ± 1.2	48.6 ± 4.4
$PheNH_2$	8.3 ± 1.0	−37.0 ± 3.8	−4.3 ± 0.2	−79.4 ± 2.4	12.6 ± 1.3	42.1 ± 4.2
$LeuNH_2$	9.3 ± 0.8	−34.4 ± 2.0	−4.2 ± 0.5	−77.6 ± 0.9	13.5 ± 1.1	43.2 ± 3.8
Leu-Ala	8.9 ± 0.8	−29.5 ± 2.9	−5.8 ± 1.9	−75.8 ± 5.8	14.8 ± 1.2	46.4 ± 4.1

[a] Units: $\Delta H^{\ddagger}$, kcal/mol; $\Delta S^{\ddagger}$, cal/mol·K. [b] $\Delta X^{\ddagger}_{III}$, $\Delta H^{\ddagger}_{II}$, and ΔX_{α} are the activation parameters corresponding to k_2/K_s, k_3/K_2K_s, and α, respectively.

partition constant for the reaction intermediate, $(E:S)_2$.

We fit the data sets of Figure 1, for FA-Gly-X-NH_2, and the data set of Figure 2C, for FA-Gly-Leu-Ala, to a thermodynamic form of eq 17 that is similar to eq 8. The parameters we solved for were $\Delta H^{\ddagger}_{II}$ and $\Delta S^{\ddagger}_{II}$, which correspond to k_2/K_3, and ΔH_{α} and ΔS_{α}, which corresponds to α. We are also interested in the activation parameters for the process governed by k_3/K_sK_2; that is, $\Delta H^{\ddagger}_{III}$ and $\Delta S^{\ddagger}_{III}$. Note that k_3/K_sK_2 is simply the product of α and k_2/K_s, and therefore, $\Delta X^{\ddagger}_{III}$ is equal to the sum of ΔX_{α} and $\Delta X^{\ddagger}_{II}$. Estimates for all these parameters are summarized in Table VIII. Values for $\Delta H^{\ddagger}_{III}$ and $\Delta S^{\ddagger}_{III}$ can also be determined directly from a fit of the data to a thermodynamic form of eq 18:

$$\left(\frac{k_c}{K_m}\right)^{-1} = \left(\frac{k_2}{K_s}\right)^{-1} + \left(\frac{k_3}{K_sK_2}\right)^{-1} \qquad (18)$$

These are the values for $\Delta H^{\ddagger}_{III}$ and $\Delta S^{\ddagger}_{III}$ that appear in Table VIII. The values of $\Delta H^{\ddagger}_{II}$ and $\Delta S^{\ddagger}_{II}$ that were generated by this fitting procedure agree with those generated above. The parameters of Table VIII were used to draw the theoretical lines through the data points of Figures 1A–C and 2C.

The parameters of Table VIII predict a temperature-dependent change in rate-limiting step that quantitatively accounts for the curved Eyring plots for k_c/K_m. At low temperature, α is less than 1 and k_c/K_m equals k_3/K_sK_2, while at high temperature α is greater than 1 and k_c/K_m equals k_2/K_s. Thus, with increasing temperature, the rate-limiting step changes from the step governed by k_3 to the step governed by k_2.

Model II can also account for several other features of thermolysin catalysis. Recall that Fukuda and Kunugi[7b] proposed a mechanism similar to model II for the thermolysin-catalyzed hydrolysis of FA-Gly-Phe-Ala. In their studies, they observed a presteady state burst prior to steady-state hydrolysis of substrate and, based on the kinetics associated with the burst phase, suggested that in addition to the initial encounter complex, $(E:S)_1$, another complex, $(E:S)_2$, forms prior to the hydrolytic step. In fact, from our data, $(E:S)_2$ appears to accumulate since K_m ($=K_sK_2 = 10^{-4}$ M) is less than K_s ($>10^{-3}$ M). The accumulation of $(E:S)_2$ requires that K_2 ($=k_{-2}/k_2$) be less than 1. If we now consider FA-Gly-$LeuNH_2$, the observation that is K_m is so much larger than the K_m for FA-Gly-Leu-Ala suggests that $(E:S)_2$ does not accumulate for FA-Gly-$LeuNH_2$ (i.e., $K_2 > 1$), and that for this substrate, K_m equals K_s.

Given that K_2 is less than 1 for FA-Gly-Leu-Ala and greater than 1 for FA-Gly-$LeuNH_2$, we can derive rate expressions for k_c, K_m, and k_c/K_m for both substrates at low temperature, where $\alpha < 1$, and at high temperature, where $\alpha > 1$. These rate expressions are summarized in Table IX and lead to the following predictions:

(1) Eyring plots for k_c/K_m should be qualitatively similar for FA-Gly-$LeuNH_2$ and FA-Gly-Leu-Ala since for both substrates k_c/K_m changes from k_3/K_sK_2 at low temperature ($\alpha < 1$) to k_2/K_s at high temperature ($\alpha > 1$). Inspection of Figures 1A and 2C verifies this prediction.

(2) Since the expressions for k_c and K_m for the hydrolysis of FA-Gly-Leu-Ala change at extremes of temperature, the Eyring plots for these parameters are predicted to be nonlinear. Parts A and B of Figure 2 demonstrate that this is the case. We were able to fit the data of Figure 2A to the thermodynamic form of eq 15. With the assumption that $K_2 < 1$ for FA-Gly-Leu-Ala, we calculate the following activation parameters for k_3 and k_2: $\Delta H^{\ddagger}_3 = 12$ kcal/mol, $\Delta S^{\ddagger}_3 = -7.8$ kcal/mol; and, $\Delta H^{\ddagger}_2 = 2.1$ kcal/mol, $\Delta S^{\ddagger}_2 = -41$ eu. These parameters confirm the prediction that k_c is rate-limited by k_3 at low temperature and k_2 at high temperature. Unfortunately, the thermodynamic form of the expression for K_m is too complex to solve by nonlinear least-squares analysis. However, we did verify that the temperature dependence of K_m can be generated from the ratio of the temperature dependencies of k_c and k_c/K_m.

Table IX. Steady-State Kinetic Predictions for the Temperature Dependence of the Thermolysin-Catalyzed Hydrolyses of FA-Gly-$LeuNH_2$ and FA-Gly-Leu-Ala

	low temp, $\alpha < 1$			high temp, $\alpha > 1$		
substrate	k_c	K_m	k_c/K_m	k_c	K_m	k_c/K_m
FA-Gly-$LeuNH_2$	k_3/K_2	K_s	k_3/K_sK_2	k_2	K_s	k_2/K_s
FA-Gly-Leu-Ala	k_3	K_sK_2	k_3/K_sK_2	βk_2[a]	βK_s[a]	k_2/K_s

[a] $\beta = k_3/(k_2 + k_3)$.

(3) For FA-Gly-$LeuNH_2$, the expression for K_m does not change at extremes of temperature. This predicts that the van't Hoff plot for K_m should be linear and reflect the simple temperature dependence of K_s. This prediction is confirmed by Kunugi et al.,[7a] who found a linear van't Hoff plot of K_i for the inhibition of thermolysin by Z-Phe-GlyNH_2 ($K_i = 10^{-3}$ M, 25 °C).

Model IIIa: Temperature-Dependent Equilibrium of Enzyme Forms; E′ is Inactive. In model IIIa, we propose that the curved Eyring plots of Figure 1 arise from a temperature-dependent equilibrium between two enzyme forms: an active form of thermolysin, E, and an inactive form of thermolysin, E′. According to this model, as the temperature increases, the equilibrium shifts to favor formation of E′. The steady-state rate expression for k_c/K_m for the mechanism of model IIIa is given in eq 19, where

$$\frac{k_c}{K_m} = \frac{k_2/K_s}{1 + K_1} \qquad (19)$$

$K_1 = [E']/[E]$. The thermodynamic form of this equation was used to fit the data of Figure 1. The parameters that we solved for are $\Delta H^{\ddagger}_{II}$ and $\Delta S^{\ddagger}_{II}$, which correspond to k_2/K_s; and ΔH_1 and ΔS_1, which correspond to K_1.

An important prediction that results from this analysis is that the magnitude of K_1 and its associated thermodynamic parameters should not be dependent on the identity of the substrate. Table X indicates that K_1 changes by over an order of magnitude with changes in substrate structure. Thus, the mechanism of model IIIa cannot be used to explain our curved Eyring plots.

Model IIIb: Temperature-Dependent Equilibrium of Enzyme Forms; E′ is Active. Model IIIb is related to model IIIa in that it involves a temperature-dependent equilibrium of two enzyme forms. However, in model IIIb, both forms are catalytically active. For this model to produce curvature, E′ must be less active than E and must increase in concentration with increasing temperature.

The steady-state rate expression for k_c/K_m for the mechanism of model IIIb is given in eq 20. When we attempted to fit the

$$\frac{k_c}{K_m} = \frac{[k_2/K_s + (k_2/K_s)']}{1 + K_1} \qquad (20)$$

data sets of Figure 1 to the thermodynamic form of eq 20, we

Table X. Activation Parameters[a,b] for the Thermolysin-Catalyzed Hydrolysis of FA-Gly-P′: Analysis According to Model IIIa

P′	$\Delta H^{\ddagger}_{11}$	$\Delta S^{\ddagger}_{11}$	ΔH_1	ΔS_1	ΔG_1[c]	K_1[c]
Ala	12	−40	18	56	1.3	0.11
Abu	12	−36	17	53	1.2	0.13
Val	13	−27	16	52	0.50	0.43
Nva	11	−33	14	48	−0.30	1.7
Phe	7	−40	12	41	−0.22	1.4
Leu	9	−36	14	44	0.89	0.23

[a] Units: $\Delta H^{\ddagger}$, kcal/mol; $\Delta S^{\ddagger}$, cal/mol·K. [b] $\Delta X^{\ddagger}_{11}$ and ΔX_1 are the activation parameters corresponding to k_2/K_s and K_1, respectively. [c] T = 298 °C for the calculation of ΔG_1 and K_1.

found that these fits would not converge. Given the complexity of the equation (i.e., three ΔH, ΔS pairs) this is not a surprising result and simply indicates that our data cannot be uniquely defined by this expression. That is, many sets of activation parameters can be found that fit our data equally well.

Despite the inability to test model IIIb quantitatively, we believe that we can exclude it on the basis of the following two facts: (1) In the temperature range used in these experiments, thermolysin displays no structural changes, as evidenced by UV and fluorescence spectral studies.[30] (2) This model predicts that van't Hoff plots of K_i for inhibition of thermolysin must be curved. There are examples of linear van't Hoff plots.[7a]

Summary

Model II is the simplest model that can explain both the results presented in this paper and the results of other investigators. Model I fails because the activation parameters that are required to fit our data are similar to those associated with large-scale protein-folding reactions. These parameters are unreasonable for catalytic events. Models IIIa and IIIb also need not be considered. The nonlinear Eyring plots predicted by these models arise due to protein structural changes of the enzyme and should therefore not be dependent on the structure of substrates or inhibitors. Since the shape of Eyring and van't Hoff plots are clearly dependent on substrate and inhibitor identity, the mechanisms of these models cannot account for our data. Furthermore, there is no evidence for protein structural changes in the temperature range that we used in our experiments.

Discussion

The temperature dependence of thermolysin catalysis was considered in some detail in the previous section and led us to the conclusion that the mechanism of model II can best accommodate our experimental results. In this section, we will use this model as the mechanistic framework for our interpretation of substrate specificity and isotope effect data.

Mechanistic Origins of Thermolysin's Substrate Specificity. One of the goals of this work was to define the mechanistic origins of thermolysin's substrate specificity. Specifically, we wish to provide a mechanistic rational for the differences in k_c/K_m that we see in Table I for substrates of general structure FA-Gly-X-NH_2, as well as for the difference in reactivity between FA-Gly-LeuNH_2 and FA-Gly-Leu-Ala. In the context of model II, we have to consider the possibility that substrate structure might influence the identity of the rate-limiting step, thereby influencing the identity and structure of the rate-limiting transition state. One way to explore this possibility is to determine if the series of reactions that we have studied obeys an isokinetic relationship.[31] This relationship is tested in Figure 3, where we plot ln $k'_{20°C}$ vs ln $k'_{50°C}$ for reaction of thermolysin with the dipeptide amides as well as with FA-Gly-Leu-Ala, and is found to be linear, with a correlation coefficient of 0.997 and a slope of 0.945 ± 0.014. The strict linearity of this relationship indicates that this series of thermolysin-catalyzed reactions does indeed obey an isokinetic relationship. This suggests that at least between 5 and 20 °C, these reactions proceed through structurally similar rate-limiting transition states.[31] It is interesting that if the data point for

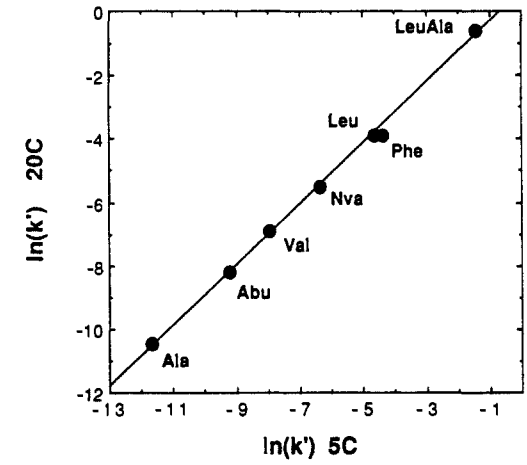

Figure 3. Isokinetic plot for thermolysin catalysis. Hydrolyses of FA-Gly-Xaa-NH_2 were conducted in a pH 6.48 buffer containing 100 mM MES and 10 mM $CaCl_2$. Values of k_c/K_m at the two indicated temperatures were multiplied by $[E]_{standard\text{-}state}$ = 10^{-6} M before plotting.

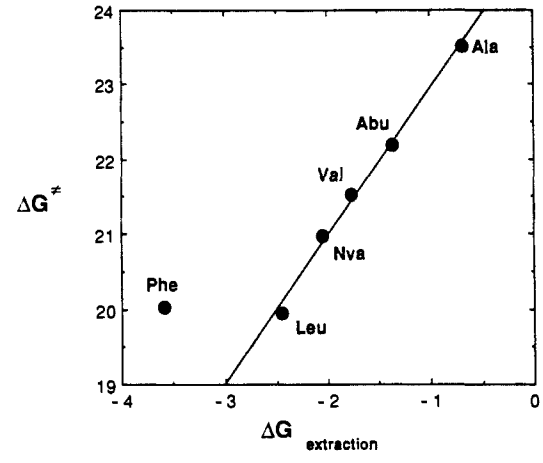

Figure 4. Correlation between P_1' side-chain hydrophobicity and free energies of activation for the thermolysin-catalyzed hydrolyses of FA-Gly-X-NH_2. Hydrolyses of FA-Gly-Xaa-NH_2 were conducted at 25 °C in a pH 6.48 buffer containing 100 mM MES and 10 mM $CaCl_2$. $\Delta G^{\ddagger}$ was calculated as $-RT$ ln $[k/(k^*T/h)]$, where T = 298 K and k = $(k_c/K_m)[E]_{standard\text{-}state}$ ($[E]_{standard\text{-}state}$ = 10^{-6} M). $\Delta G_{extraction}$ are the free energies of extraction of the amino acid side chains from water into *n*-octanol.[32]

FA-Gly-PheNH_2 is excluded, the correlation coefficient increases to 0.999 and the relative standard deviation of the slope decreases from 1.48% to 1.05% (slope = 0.954 ± 0.010). Admittedly, these are modest differences, but they suggest that FA-Gly-PheNH_2 may be an outlier in this correlation. The mechanistic significance of FA-Gly-PheNH_2 being an outlier is discussed later in this section.

Having established that thermolysin-catalyzed hydrolyses of dipeptide amides proceed through structurally similar transition states, it remains for us to determine the origin of the reactivity differences among these substrates. Inspection of Table I reveals that a correlation might exist between k_c/K_m and the hydrophobicity of the P_1' side chain. This relationship is confirmed and quantitated in Figure 4, where we find that $\Delta G^{\ddagger}$, the free energy of activation, correlates linearly (slope = 1.96; r^2 = 0.994) with $\Delta G_{extraction}$, the free energy of extraction of the amino acid side chain from water into *n*-octanol.[32]

Again, we see that FA-Gly-PheNH_2 is an "outlier". The correlation predicts an activation energy for this substrate (17.8 kcal/mol) that is 2.2 kcal/mol lower than the observed activation energy (20.0 kcal/mol) and, thus, a value for k_c/K_m (600 000 M^{-1} s^{-1}) that is 40 times greater than experiment. This indicates that

(30) Ohta, Y. *J. Biol. Chem.* **1967**, *242*, 509–515.
(31) Exnor, O. *Prog. Phys. Org. Chem.* **1973**, *10*, 411–482.
(32) Hansch, C.; Coats, E. *J. Pharm. Sci.* **1970**, *59*, 731–748.

hydrophobicity cannot entirely account for thermolysin's P_1' specificity and that there must be other factors that play a part in determining P_1' specificity. X-ray crystallographic[2] and modeling[5] studies suggest that the shape of the S_1' subsite may not allow efficient transition-state binding of amino acid side chains larger than the isobutyl group of Leu. This and the observation that FA-Gly-PheNH_2 is an outlier in the isokinetic relationship suggest that transition-state interactions between thermolysin and FA-Gly-PheNH_2 are not the same as those between thermolysin and other substrates in this series.

The other aspect of thermolysin's substrate specificity that we will consider is the 30-fold increase in k_c/K_m that is observed when FA-Gly-LeuNH_2 is extended to FA-Gly-Leu-Ala. To try to understand this rate enhancement, steady-state rate constants, k_c and K_m, were determined for these substrates and are summarized in Table II. Curiously, when the 30-fold increase in k_c/K_m is dissected into individual contributions from k_c and K_m, we find greater than 150- and 5-fold decreases in K_m and k_c, respectively. The explanation for these decreases in K_m and k_c lies in the stabilization that $(E:S)_2$ realizes when thermolysin reacts with the extended substrate, FA-Gly-Leu-Ala. This is illustrated below for the case $\alpha < 1$ (see the steady-state kinetic expressions of Table IX).

For FA-Gly-LeuNH_2, K_m reflects only the accumulation of $(E:S)_1$, while for FA-Gly-Leu-Ala, K_m reflects accumulation of $(E:S)_2$. This situation reflects the greater stability of $(E:S)_2$ relative to $(E:S)_1$ when S is FA-Gly-Leu-Ala and thus explains the decrease in K_m for FA-Gly-Leu-Ala relative to FA-Gly-LeuNH_2. If we now consider k_c, we see that, for FA-Gly-LeuNH_2, this parameter reflects the energy difference between $(E:S)_1$ and the transition state for k_3, while for FA-Gly-Leu-Ala, k_c reflects the energy difference between $(E:S)_2$ and the same transition state. For FA-Gly-Leu-Ala, the stabilization experienced by $(E:S)_2$ is *not* manifested in the transition state for k_3: binding energy is utilized for the ground-state stabilization of $(E:S)_2$ and not for transition-state stabilization. Thus, k_c for FA-Gly-LeuNH_2 is greater than k_c for FA-Gly-Leu-Ala.

Isotope Effects and Transition-State Structural Features for Reactions of Thermolysin. To probe structural features of the rate-limiting transition state for the process governed by k_c/K_m we determined β-deuterium and solvent deuterium isotope effects for several thermolysin-catalyzed reactions. In this section, we will demonstrate that these isotope effects support the mechanism of model II.

β-Deuterium isotope effects on k_c/K_m for the thermolysin-catalyzed hydrolyses of FA-Gly-LeuNH_2 and FA-Gly-Leu-Ala are summarized in Table III. As we pointed out in Results, these isotope effects do not depend on substrate structure or pH and give an average value of 0.97 ± 0.01. This value indicates that the vibrational force field associated with the methylene hydrogens of glycine is stronger in the rate-limiting transition state than in the ground state.[33,34] Together with the knowledge that the ground state for the process governed by k_c/K_m is substrate free in solution, the isotope effect provides structural information about the rate-limiting transition state. In the framework of carbonyl addition reactions, an inverse β-deuterium isotope effect suggests a partially sp^3-hybridized, tetrahedral intermediate-like transition state. The origin of β-deuterium isotope effects is usually explained in terms of hyperconjugation.[33,34] The hyperconjugation between the β-hydrogens and carbonyl moiety of the glycine is reduced as the substrate progresses from an sp^2-hybridized ground state to the sp^3-hybridized transition state. It is the loss of hyperconjugation in the transition state that strengthens the force field associated with the hydrogens of glycine and causes the inverse effect.

The theoretical limit for β-deuterium isotope effects in carbonyl addition reactions is about 0.96 per β-D or, for the two labeled hydrogens of glycine, about $(0.96)^2$ or 0.92.[33,34] Our experimental value of only 0.97 suggests that one of two possible situations is operating: (1) The transition state does not have much tetrahedral character. The observed isotope effect of 0.97 would be the actual, "intrinsic" isotope effect[35] for this process. If formation of the tetrahedral intermediate is rate-limiting, this requires an early transition state; while if decomposition of the tetrahedral intermediate is rate-limiting, this requires a late transition state. Or (2), the transition state that we observe experimentally is actually a "virtual" transition state[25,26] with structural contributions from at least two partially rate-limiting real transition states. In this case, the isotope effect is the weighted average of the isotope effects for the several partially rate-limiting processes. Of the two mechanistic alternatives, the second alternative seems more likely, since a temperature-sensitive virtual transition state is predicted by model II. And, indeed, this prediction is borne out by the data of Table VI, where we observe that as the temperature rises, and k_3 becomes less rate-limiting, the β-deuterium isotope effect approaches unity.

The temperature dependence of the β-deuterium isotope effects is consistent with a mechanism in which the second step of the reaction of model II is a conformational change of the Michaelis complex with an isotope effect near 1.0. According to this mechanism, the third step of the reaction would reflect the actual hydrolysis of the amide bond with an inverse β-deuterium isotope effect near 0.94. The assignment of the second and third steps of the reaction to conformational and chemical changes is also consistent with the activation parameters that we determined for FA-Gly-Leu-Ala. In the previous section, we calculated that for k_2 and k_3 $\Delta H^{\ddagger}_2$ = 2.1 kcal/mol, $\Delta S^{\ddagger}_2$ = −41 eu, $\Delta H^{\ddagger}_3$ = 12 kcal/mol, and $\Delta S^{\ddagger}_3$ = −7.8 kcal/mol.

An inverse β-deuterium isotope effect tells us that, in the rate-limiting transition state of the process governed by k_3/K_sK_2, the carbonyl group of the scissile bond has tetrahedral character and is partially sp^3-hybridized. Therefore, the rate-limiting step for k_3/K_sK_2 must be either the formation or the decomposition of the tetrahedral intermediate formed from the addition of the

Scheme III. Mechanisms of Amide Hydrolysis by Thermolysin

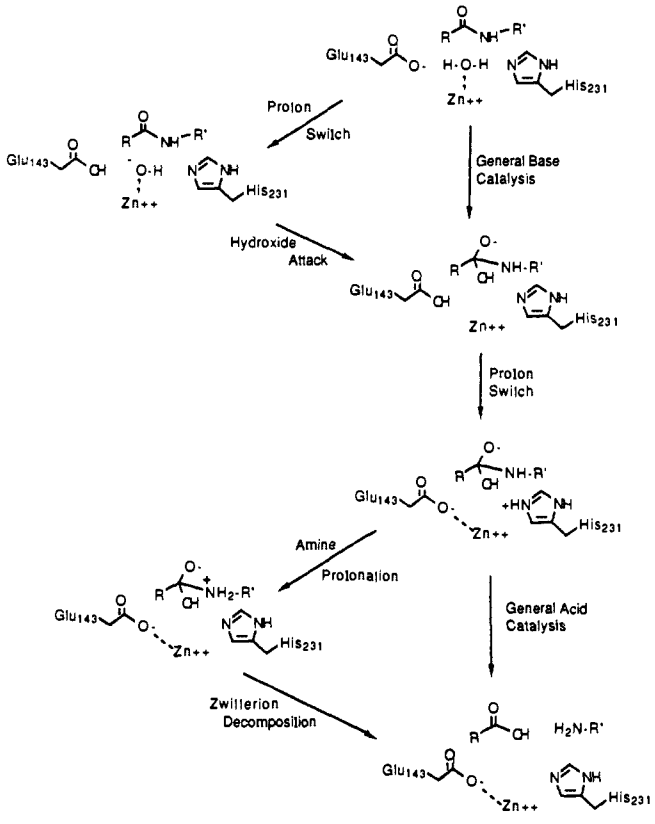

(33) Hogg, J. L.; Rodgers, J.; Kovach, I. M.; Schowen, R. L. *J. Am. Chem. Soc.* **1980**, *102*, 79–85.

(34) Kovach, I. M.; Hogg, J. L.; Raben, T.; Halbert, K.; Rodgers, J.; Schowen, R. L. *J. Am. Chem. Soc.* **1980**, *102*, 1991–1999.

(35) Northrop, D. B. *Biochemistry* **1975**, *14*, 2644–2652.

zinc-bound water molecule. It is still unclear which of these steps is rate-limiting to k_3. Potential mechanisms for the chemistry of k_3 are shown in Scheme III.

Formation of the tetrahedral intermediate can occur either through a general-base mechanism, catalyzed by Glu_{143}, or through attack of zinc-bound hydroxide, formed via a proton switch from $Zn-OH_2$ to Glu_{143}.[36] Decomposition of the tetrahedral intermediate can then occur either through a general-acid mechanism, catalyzed by the imidazolium moiety of His_{231}, or through decomposition of a zwitterionic intermediate, formed via a rapid preprotonation step.

In an attempt to determine which of these steps rate-limits k_3 and, in general, to further characterize the structure of the rate-limiting transition state, we determined a series of solvent deuterium isotope effects. These isotope effects were for k_c/K_m and were done for the hydrolyses of FA-Gly-Leu-Ala and the substrate series FA-Gly-X-NH_2 (Table IV), as well as for FA-Gly-Leu-NH_2 as a function of temperature (Tables VI).

The solvent isotope effects that we determined are all inverse and, to a first approximation, equal 0.74. This value stands in marked contrast to solvent isotope effects for reactions catalyzed by serine protease,[37] which typically range from 2.5 to 3.5 and reflect the general-acid/general-base catalysis that promotes acyl transfer to and from the active-site serine. The isotopic silence that we observe for thermolysin indicates an absence of protolytic catalysis in the transition state for k_c/K_m and allows us to rule out the two general-catalyzed steps of Scheme III as well as the proton switch and amine protonation steps. Rate limitation of k_3 by one of these reaction steps would manifest itself in a large, normal solvent isotope effect on k_c/K_m, since in the transition states for all of these processes, a proton would be "in flight".

To further interpret the observed isotope effect of 0.74, we start with the general expression of eq 21,[37] which expresses the observed

$$^{D_2O}k_{obs} = \frac{\prod\Phi_{reactant}}{\prod\Phi_{\neq}} \quad (21)$$

solvent isotope effect, $^{D_2O}k_{obs}$, as the ratio of products of reactant-state and transition-state fractionation factors for all exchangeable hydrogens, $\Phi_{reactant}$ and $\Phi_{\neq}$, respectively. For the reactions under consideration here, we expand eq 21 to

$$^{D_2O}k_{obs} = \frac{(\Phi_{Zn-OH_2})^2[\prod\Phi_{FA\text{-}Gly\text{-}LeuNH_2}][\prod\Phi_{thermolysin}]}{\prod\Phi_{\neq}} \quad (22)$$

where Φ_{Zn-OH_2} is the fractionation factor for one of the two hydrogens of the zinc-bound water molecule and $\prod\Phi_{FA\text{-}Gly\text{-}LeuNH_2}$ and $\prod\Phi_{thermolysin}$ are the products of fractionation factors for the substrate and enzyme, respectively.

If we make the reasonable assumptions that the fractionation factors for the substrate, enzyme, and transition state are unity[37] and set Φ_{Zn-OH_2} equal to 0.85,[38,39] we can calculate a value for $^{d_2O}k_{obs}$ of 0.72. This calculation agrees well with our experimental value of 0.74 and supports a mechanism in which the zinc-bound water molecule of uncomplexed thermolysin $[(\Phi_{Zn-OH_2})^2 = 0.72]$ undergoes reaction with substrate to become part of a tetrahedral addition adduct with a fractionation factor of unity.[37]

The dependencies of $^{D_2O}k_{obs}$ on substrate structure (Table IV) and temperature (Table VI) are more difficult to interpret. Neither of these dependencies appears to fit virtual transition-state predictions of model II. That is, there is no obvious correlation between $^{D_2O}k_{obs}$ and α for the substrates of Table IV, nor can the solvent isotope effect data of Table VI be fit to eq 20. Concerning the first point, it is not clear that α should be expected to correlate with $^{D_2O}k_{obs}$. Implicit in the expectation of such a correlation is the assumption that the force fields associated with exchangeable protons will be identical for all substrates in their enzyme-bound transition states. However, at the present time, there is no way to predict the dependence of the intrinsic solvent isotope effect on structural features of the transition state and, thus, on structural features of the substrate. The second point, the inability of the temperature dependence of $^{D_2O}k_{obs}$ to be fit by eq 20, may suggest that model II is not an accurate representation of thermolysin's mechanism. Although more complex mechanisms can be formulated that accommodate the temperature dependence of $^{D_2O}k_{obs}$, we do not feel justified in proposing these mechanisms since they would be based on a single anomalous result.

Summary. The results of this study suggest that thermolysin-catalyzed reactions follow a sequential mechanism in which the Michaelis complex changes conformation before the chemical steps of peptide bond hydrolysis. k_c/K_m for these reactions is partially rate-limited by both the conformational change and the hydrolysis step. The extent to which either of these steps limits the rate is dependent on temperature, with chemistry contributing more to rate limitation at lower temperature. The chemical step, which corresponds to formation and decomposition of a tetrahedral intermediate, is itself rate-limited by a reaction step that does not involve protolytic catalysis. Likely candidates for this step are addition of a zinc-bound hydroxide to the substrate carbonyl carbon or decomposition of a zwitterionic tetrahedral intermediate. Although the experiments of this study do not allow us to discriminate between these two alternatives, we favor the latter based on the pH dependence of k_c/K_m, which suggests the catalytic importance of both Glu_{143} and His_{231}.[7,40]

(36) Valle, B. L.; Galdes, A. *Adv. Enz. Relymol. Relat. Areas Mol. Biol.* **1984**, *56*, 283–430 (especially pp 408–411).
(37) Venkatasubban, K. S.; Schowen, R. L. *CRC Crit. Rev. Biochem.* **1985**, *17*, 1–41.
(38) Kassebaum, J. W.; Silverman, D. N. *J. Am. Chem. Soc.* **1989**, *111*, 2691–2696.
(39) Schmidt, J.; Chen, J.; DeTraglia, M.; Minkel, D.; McFarland, J. T. *J. Am. Chem. Soc.* **1979**, *101*, 3634–3670.
(40) Izquierdo, M. C.; Stein, R. L., unpublished data.